

Temperature and composition dependence of the Soret coefficient in Lennard-Jones mixtures presenting consolute critical phenomena

Erminia Leonardi, Bruno D'Aguanno, and Celestino Angeli

Citation: *The Journal of Chemical Physics* **132**, 124512 (2010); doi: 10.1063/1.3367930

View online: <http://dx.doi.org/10.1063/1.3367930>

View Table of Contents: <http://scitation.aip.org/content/aip/journal/jcp/132/12?ver=pdfcov>

Published by the [AIP Publishing](#)

Advertisement:



Re-register for Table of Content Alerts

Create a profile.



Sign up today!



Temperature and composition dependence of the Soret coefficient in Lennard-Jones mixtures presenting consolute critical phenomena

Erminia Leonardi,^{1,a)} Bruno D'Aguanno,¹ and Celestino Angeli²¹CRS4, Center for Advanced Studies, Research and Development in Sardinia, Parco Scientifico e Tecnologico, POLARIS, Edificio 1, 09010 Pula, Italy²Dipartimento di Chimica, Università di Ferrara, Via Borsari 46, I-44100 Ferrara, Italy

(Received 18 December 2009; accepted 26 February 2010; published online 31 March 2010)

Nonequilibrium molecular dynamics calculations have been carried out on Lennard-Jones binary mixtures with the aim to investigate the dependence of the Soret coefficient on the temperature and on the composition for systems presenting phase transitions. By an appropriate choice of the cross interaction parameter, ϵ_{12} ($0 < \epsilon_{12} < \min\{\epsilon_{11}, \epsilon_{22}\}$), these systems show a mixing/demixing (consolute) phase transition. The other parameters are those of a binary mixture of Argon and Krypton. This system has been considered over a wide range of temperatures (up to ≈ 1000 K), of compositions ($0.1 \leq x_1 \leq 0.9$), and of cross interaction parameter ($0 < \epsilon_{12} < \min\{\epsilon_{11}, \epsilon_{22}\}$). The study allows the formulation of a very simple expression for the Soret coefficient, S_T , as a function of temperature and composition. Indeed the computed values of S_T in the one phase region outside the critical region are closely fitted by the function $[T - T_c(x_1)]^{-1}$ where $T_c(x_1)$ is the demixing temperature of the mixture under study. This result indicates for this type of systems a dependence of S_T , as a function of the temperature, on a unique characteristic property of the fluid mixture, the demixing temperature T_c , which, in turn, is a function of the binary mixture composition x_1 . © 2010 American Institute of Physics. [doi:10.1063/1.3367930]

I. INTRODUCTION

Thermodiffusion, also called the Ludwig–Soret effect,^{1,2} is a nonequilibrium effect that describes the coupling between a temperature gradient and an induced resulting mass flux, which adds up to the Fickian flux, in a multicomponent system. In the presence of a constant temperature gradient, in order to reach a steady state, a concentration gradient must develop. The amplitude of the concentration gradient at the steady state is controlled by the Soret coefficient, $S_T = D_T/D$ (D and D_T are the Fickian and the thermal diffusion coefficients, respectively). In a binary mixture of molar fraction x_1 for species 1 and for fluxes in the z -direction, the Soret coefficient can be expressed as

$$S_T = \frac{D_T}{D} = - \frac{1}{x_1(1-x_1)} \left(\frac{\partial x_1}{\partial z} \right) \left(\frac{\partial T}{\partial z} \right)^{-1}, \quad (1)$$

where the gradients are evaluated at the steady state. Positive values of S_T indicate that species 1 tends to accumulate in the “cold” region. It is common practice to choose as species 1 the heavier species. With this notation, in many cases S_T has a positive value in accordance with the dilute gases result.³ For instance, polymers in solution conform to this rule with relatively few known exceptions.

An exhaustive analysis of the literature concerning the Soret effect is beyond the aim of the present paper. A discussion on some relevant previously published studies on the thermodiffusion process can be found in recent reviews^{4,5} and in a paper of our group,⁶ to which the reader is referred,

and we limit ourselves to report here the key points. As mentioned in various papers, thermodiffusion is an hydrodynamic transport mechanism that continues to lack of a simple physical explanations,⁷ although it is now accepted that it is influenced from both kinetic and thermodynamic contributions. Such contributions depend on the particle mass, on the nature and form of the interaction potential, and on the concentration of the components. In particular, it is worth remembering that from the kinetic theory of dilute gasses, it appears that S_T is more dependent on the details of the interaction potential than other transport properties^{3,8} (see also Refs. 9 and 10 for two recent papers concerning colloidal suspensions). For this reason various authors have published studies concerning the dependence of S_T on the potential parameters.^{6,11} Indeed, the understanding of the thermodiffusion process can take advantage from the knowledge of the dependence of S_T on the temperature (and possibly on other physical quantities describing the system) for different interaction potentials, while for ideal gas mixtures it is known that $S_T = 1/T$. The details of the physical system also control the behavior of S_T as a function of the temperature, especially in the so-called crossover critical regions.¹² Expressions for the dependence of S_T on T on moving in the rich phase diagram of binary mixtures¹³ are lacking, too.

Müller–Plathe^{11,14} carried out a study concerning the thermal diffusion in high density liquids, which is of particular importance for the work presented here. In particular, he proposed a nonequilibrium molecular dynamics (NEMD) method for generating temperature gradients by imposing a heat flux, initially indicated with “reverse-NEMD” (RNEMD) and then with “boundary-driven-NEMD”

^{a)}Author to whom correspondence should be addressed. Electronic mail: ermy@crs4.it.

(boundary-NEMD). For the sake of conciseness we shall use in the following the acronym RNEMD. In summary, in this method the energy flux is generated by exchanging, for each species, the velocity vectors of the hottest particle in the cold region with the coldest one in the “hot” region. This leads to an energy transfer from the cold region to the hot one if the coldest particles of the hot region has less kinetic energy than the hottest one of the cold region (due to the broad form of the Maxwell–Boltzmann distribution this hypothesis is normally satisfied). As a consequence of this artificial energy flux, a temperature gradient develops between the hot and the cold regions until a steady state is reached in which the energy flux due to the temperature difference compensates the artificial flux. This method, which has been implemented in our laboratory into the commercial code M.DYNAMIX,¹⁵ has been used in our previous work⁶ and is adopted also in the present study. Details of the method can be found in the original papers, in Ref. 6, and in Sec. II.

By using this algorithm, Müller–Plathe and collaborators have studied both qualitative and quantitative aspects of the thermal diffusion process, investigating the influence of systematic variations of the physical parameters (mass, atomic diameter, interaction strength)^{11,16} in binary mixtures described by Lennard-Jones (LJ) potentials. With the aim to contribute to the process toward a definition of a model of the thermodiffusion process, in a previous paper⁶ we have studied the influence on the thermodiffusion coefficient of both the temperature and the softness of the interaction potential. In that case the potential used, $(\sigma/r)^n$, was derived from the LJ one, by neglecting the attractive part and systematically changing the exponent n of the repulsive term. In particular, we had chosen an equimolar binary mixture of particles, with LJ parameters (mass, σ and ϵ) corresponding to those of Argon and Krypton. The study has shown an almost ideal behavior for $n \geq 3$, while for $n=1$ a peculiar dependence of S_T on T (with a sign change) has been found.

The aim of this work is to further proceed in this research project, by presenting a study concerning the evaluation of the dependence of S_T on both the temperature and the composition, in the case of binary LJ mixtures in a range of temperature and composition ending on the line of consolute critical points. Such a line is a liquid-liquid equilibrium line and, in a PT phase diagram of a binary mixture, it is only one of the possible phase equilibrium lines, the others being liquid-vapor critical lines and three phase equilibrium lines (coexistence of two liquid phases and a vapor phase), as well illustrated by Anisimov *et al.*¹³ In further work, we plan to extend this methodology to other mixtures and to other regions of the phase diagram, such as those close to the line of liquid-vapor critical points.

By considering the line of critical consolute temperatures, T_c , as a reference, one can identify two regions. In the first region (called critical domain, usually few kelvin, or less, around T_c), the divergence of the correlation length of the fluctuations leads to universal scaling laws for the critical behavior of the transport coefficients.¹² While D_T does not show a critical behavior, D presents the characteristic asymptotic (Ising-like) critical slowing down¹⁷ approaching T_c , leading to an asymptotic divergence of the Soret coefficient

TABLE I. LJ parameters for Argon and Krypton (from Ref. 11).

Atom(type)	m (amu)	σ (Å)	ϵ (kJ/mol)
Kr(1)	83.80	3.633	1.39
Ar(2)	39.95	3.405	1.00

such as $(T-T_c)^{-0.67}$ (see, for instance, Refs. 18 and 19). The second region, situated outside the critical region, is characterized by the fact that the relevance of the fluctuations becomes vanishing, the correlation length is smaller than the characteristic length scale, and the behavior is not universal, showing a marked dependence on the nature of the interacting details (classical mean field, or van der Waals, regime). In 2004 Enge and Köhler¹⁹ indicated, for the classical mean field regime, the scaling $S_T \approx \epsilon^{-1}$ where $\epsilon = (T-T_c)/T_c$. This result is obtained starting from the long-wavelength limit of the collective diffusion coefficient, considering the thermal activated nature of the background part (the one surviving in the classical mean field regime) of D and D_T and supposing that both the background contribution of the Onsager coefficient (α^b) and D_T have a similar activation energy $k_B T_a$. The $(T-T_c)^{-1}$ behavior has been experimentally confirmed^{17,19} for a polymer blend for large values of ϵ . It is important to note that this result indicates a scaling behavior and not the absolute amplitude of the effect.

Here, we report the calculation of the dependence of S_T on T and x_1 in the classical mean field regime for binary liquid mixtures of LJ particles. The study of these systems has revealed an interesting dependence of S_T on T in which the demixing temperature plays a central role.

The rest of the paper is organized as follows: in Sec. II the computational details are described and general considerations regarding the extraction of S_T from the MD simulation data are reported; in Sec. III the influence of the variation of ϵ_{ij} and of the temperature on the value of the Soret coefficient S_T is studied for an equimolar mixture of Argon and Krypton-like particles at a reduced density equal to 0.73; in Sec. IV the same equimolar mixture is analyzed at a lower density; in Sec. V the dependence of S_T on the composition is analyzed; and finally in Sec. VI we shall summarize the relevant results here obtained.

II. COMPUTATIONAL DETAILS

All simulations are performed considering a mixture of two species only, with 1500 LJ atoms, whose interacting potential is defined as

$$U_{ij}^n(r_{ij}) = 4\epsilon_{ij} \left[\left(\frac{\sigma_{ij}}{r_{ij}} \right)^{12} - \left(\frac{\sigma_{ij}}{r_{ij}} \right)^6 \right]. \quad (2)$$

In this equation σ_{ij} is the distance at which the potential changes sign, ϵ_{ij} is the depth of the potential, and r_{ij} is the distance between particles i and j .

Hereafter species 1 refers to Krypton-like atoms. The parameters of the like interactions, σ_{11} , ϵ_{11} , σ_{22} , and ϵ_{22} , are those of Krypton and Argon,¹¹ respectively, and are reported in Table I for the sake of completeness. For the interaction

potential between unlike species, while σ_{12} is computed using the Lorentz–Berthelot mixing rule

$$\sigma_{12} = (\sigma_1 + \sigma_2)/2 \quad (3)$$

in all simulations, ϵ_{12} is varied following the relation:

$$\epsilon_{12} = f\epsilon_{11}, \quad (4)$$

with f assuming values assuring that $\epsilon_{12} < \min\{\epsilon_{11}, \epsilon_{22}\}$ and therefore that the system presents a mixing/demixing (M/D) phase transition.²⁰ In particular, a series of simulations on an equimolar mixture has been performed with f ranging from 0.2 to 0.7 with an increment of 0.1. The dependence of S_T on T at $x_1=0.5$ and $f=0.6$ has been computed at two different densities. Moreover, for the case with $f=0.6$, another series of simulations has been performed varying the mixture composition from $x_1=0.1$ to $x_1=0.9$, with an increment of 0.1.

In RNEMD the simulation box has been divided into $N_s=12$ slabs of equal thickness, orthogonal to the z -direction. Slab 0 is defined as the cold slab, and slab $N/2$ as the hot slab. Such a choice allows the periodic boundary conditions to be satisfied. The value of N_s has been chosen so that reasonable statistics can be expected inside the slabs: on average there are 125 particles in each slab. The heat flux is generated by exchanging, for each species, the velocity vectors of the hottest particle in the cold slab with the coldest one in the hot slab. As discussed in Sec. I, in the hypothesis that the coldest particles of the hot slab has less kinetic energy than the hottest one of the cold slab (normally satisfied, due to the broad form of the Maxwell–Boltzmann distribution), the exchange leads to an energy transfer from the cold slab to the hot one. The temperature therefore increases in the hot slab and decreases in the cold slab. The consequence is to establish a temperature difference between the two slabs and a temperature gradient in the intermediate region. At the steady state the (artificial) energy transfer is balanced by the heat flux from the hot slab to the cold one originated by the temperature gradient. The velocity exchange is done every N_{exch} simulation time steps, where N_{exch} is chosen (in a trial and error strategy) so that the temperature gradient is as small as possible with the constraint to show a clear (and numerically stable) concentration gradient. Moreover, the value of N_{exch} is calibrated in order to produce temperature gradients similar in all simulations. This exchange algorithm can present problems in case of dilute gaseous mixtures due to the possibility that in one of the two exchanging slabs (cold and hot) a given component is absent. In the simulations here reported such a problem has not been met. Because of the symmetry of the simulation box, average values of temperature and composition are calculated between slab $N_s/2-i$ and $N_s/2+i$, with $i=1,5$, having excluded the first (0) and central (6) slabs because of the unphysical effects they can present due to the particle exchange procedure.

The RNEMD simulation, on which statistic information are collected, is always performed after two runs. The first one is an equilibrium MD (EMD) simulation 2×10^6 time steps long (in all simulations here reported $\Delta t=1$ fs) and the second one is a RNEMD simulation, other 2×10^6 time steps long. In this way we are sure that the system in the final RNEMD simulation is at the steady state. This assumption

has been verified by analyzing the behavior of the time evolution of the total energy and of the temperature and composition profiles, which is expected to be constant during the final RNEMD simulation. In the final RNEMD calculation, data are collected over a simulation 14×10^6 time steps long.

A particular role is played by the temperature used in the EMD simulation because it represents the temperature around which the temperature gradient develops, that is a sort of average temperature in the RNEMD steps. This temperature is indicated in the following with T_{eq} . RNEMD simulations have been performed at a series of values of T_{eq} , to the aim of covering a wide range of temperatures (from about 250 to 1000 K) and to have the thermodiffusion coefficient as a function of the temperature.

Some considerations are in order at this point, concerning the way used in this work for the extraction of S_T from the simulation data. The phenomenological equation governing the mass diffusion of species 1 in presence of the thermodiffusion process is

$$J_1 = -D\rho \left[\left(\frac{\partial w_1}{\partial z} \right) + S_T w_1 (1 - w_1) \left(\frac{\partial T}{\partial z} \right) \right], \quad (5)$$

where D is the Fickian diffusion coefficient, the temperature gradient and the flux J are assumed in the z -direction, ρ is the average mass density, and $w_1 = x_1 m_1 / (x_1 m_1 + x_2 m_2)$ is the weight fraction of species 1 (x_k denoting the mole fraction of species k). Under the effect of a constant temperature gradient, the system reaches a nonequilibrium steady state ($J_1=0$), and a stable concentration profile is therefore established so that Eq. (5) reduces to

$$\left(\frac{\partial w_1}{\partial z} \right) + S_T w_1 (1 - w_1) \left(\frac{\partial T}{\partial z} \right) = 0. \quad (6)$$

Taking into account the relationship between the weight fractions and the molar fractions (a quantity experimentally more accessible), we finally arrive to the expression of the Soret coefficient given by Eq. (1).

With respect to other published works, the strategy proposed by our group⁶ for the extraction of S_T from the RNEMD simulation data renounces to the request for the composition profile to be linear. A detailed description of the calculation of the Soret coefficient from the concentration and temperature profiles is given by Leonardi *et al.*⁶ and we give here only a short summary. In RNEMD the temperature and the composition profiles are known for a set of z values corresponding to the center of each slab of the simulation box. In order to carefully fit both the concentration and the temperature profiles, without assuming for them a linear behavior, very stable values of x_1 and T for each slab are necessary. For this reason less slabs and more particles (both choices increasing the number of particles for each slab) than recommended have been considered, and a rather long simulation time has been used. Within this strategy one can explore the possibility to have nonlinear concentration profiles. In particular a marked nonlinearity in concentration profile indicates that S_T shows significant changes in the range of

temperature and/or concentration found in the system and in a single simulation one can expect to have more information on the dependence of S_T from T and x_1 .

Once $T(z)$ and $x_1(z)$ are known from the analytic fitting of the RNEMD values, Eq. (1) allows the definition of S_T for each value of z_i (the center of slab i) through the analytical derivatives with respect to z of $T(z)$ and $x_1(z)$ computed in z_i and by using the value $x_1(z_i)$. One can thus obtain S_T for each couple $T(z_i)$ and $x_1(z_i)$ in the ranges $T_{\max}-T_{\min}$ and $x_1^{\max}-x_1^{\min}$, where T_{\max} and T_{\min} (x_1^{\max} and x_1^{\min}) are the maximum and minimum temperatures (molar fraction) found in the various slabs.

In order to clarify how the fitting function for the composition profile has been chosen, the first step is the integration of Eq. (1). In the hypothesis that S_T depends only on T (not strictly valid in this present work), Eq. (1), written with x_1 as the unknown function, can be integrated obtaining⁶

$$x_1(T) = \frac{1}{1 + Ae^{\int S_T dT}}, \quad (7)$$

with the parameter A defined by a boundary condition (for instance, the value of the integral of x_1 over the full interval of z , or the value of x_1 at a given z). From this equation $x_1(z)$ can be easily found if $T(z)$ is known, and one notes that $x_1(z)$ is not a linear function of z even if S_T is constant and $T(z)$ is a linear function of z . Therefore there is no reason to expect a linear composition profile in the RNEMD simulations. Referring to our previous work (Ref. 6), the nonlinear shape of the composition profile has been exploited in a recent study on binary mixtures of hard spheres.²¹

Let us note that, if S_T has the form $(T-B)^{-1}$ (that actually found in the simulation hereafter described), one has

$$x_1(T) = \frac{1}{A' - B'T}, \quad (8)$$

where A' and B' are two constants related to A and B . If the temperature profile is linear in z (as always found in our simulations), one can eventually write

$$x_1(z) = \frac{1}{a - bz}. \quad (9)$$

This expression has been used to fit the x_1 values computed in the RNEMD simulations. It is worth noticing that the dependence of x_1 on z can be obtained only once the dependence of S_T on T is known, but this is actually the final result of the full procedure. One can therefore start the procedure with a reasonable fitting function for x_1 (for instance, a polynomial in z) then compute S_T at different temperatures, and only when an indication of the dependence of S_T on T is obtained, the form of $x_1(z)$ can be guessed.

A comment is in order at this point: it is implicit in the thermodynamic description of irreversible processes that the gradients are “macroscopic” in the sense that the sensible changes in the variables are produced at scales much larger than the density correlation length, which is of molecular dimensions far from the critical point. The simulation box here considered is small from this point of view, and therefore the gradients should be the smaller the possible not to

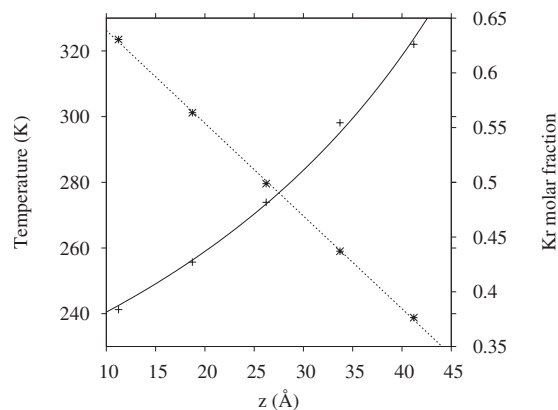


FIG. 1. Temperature and composition profiles for the equimolar mixture of Ar- and Kr-like particles for the case with $f=0.6$ and $T_{\text{eq}}=280$ K. The fitting parameter of $x_1(z)=1/(a+bz)$ are $a=2.954\ 22$ and $b=-0.033\ 256$ (rms = root-mean-square of the residuals = 0.006), while for the temperature, $T(z)=c+dz$, $c=354.494$, and $d=-2.8251$ (rms = 0.81).

enter in a regime where the validity of Eq. (5) could be questioned. Therefore, the applicability of this method, at least formally, is restricted to weak nonlinearities.

III. EQUIMOLAR MIXTURE OF ARGON- AND KRYPTON-LIKE PARTICLES AT $\rho=1.91$ g/cm³

The system is composed of 750 Argon atoms and 750 Krypton atoms in an orthorhombic periodic cell of size $89.89 \times 29.96 \times 29.96$ Å³, which corresponds to a dense liquid state, far from the triple point of both Argon (83.81 K and 0.68 atm) and Krypton (115.75 K and 0.72 atm). The volume is kept constant for all simulations, and the pressures coming out from the NVT-MD simulations range from about 2500–8000 atm in the range of temperatures considered (from about 250 to 1000 K). The time step Δt is 1 fs, and the chosen cutoff distance, $r_c=14.9$ Å, corresponds to an energy truncation, E_c , of the order of 10^{-4} kJ/mol.

In the range of temperatures explored in our simulations, the concentration profiles were always well fitted with the function reported in Eq. (9), as shown, for instance, in Fig. 1 for the case of $f=0.6$ and $T_{\text{eq}}=280$ K. For each value of the parameter f , various RNEMD simulations have been performed, spanning a wide range of temperatures T_{eq} , thus obtaining the dependence of S_T on T .

Starting from high temperatures and lowering T , S_T has been found to show in all cases the same behavior. It has always positive values, it increases as the temperature is lowered, and finally, it diverges. This behavior is well fitted by the function $1/(T-\tilde{T})$ for all value of the parameter f , as clearly shown in Fig. 2, where all values of S_T discussed in this section are reported. The inset of this figure evidently shows that for all f , there is a linear correlation, with a slope equal to -1 , of $\log(S_T)$ with respect to $\log(T-\tilde{T})$. The values of the fitting parameter \tilde{T} for the different values of f are reported in Table II.

In order to better understand the physical meaning of the temperature \tilde{T} at which the Soret coefficient diverges, equi-

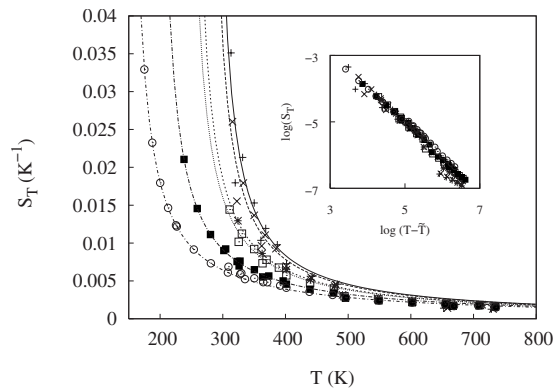


FIG. 2. Dependence of the Soret coefficient on the temperature at various values of the parameter f . Symbols: RNEMD values; lines: analytic fitting functions. The first line from the right corresponds to $f=0.2$. The other lines to 0.1 increments of f and the last line (the first from the left) to $f=0.7$. The inset reports the dependence of the logarithm of the Soret coefficient on $\log(T-\tilde{T})$.

librium molecular dynamics simulations have been performed for each value of the parameter f on a range of temperature around \tilde{T} .

Before discussing how the phase stability of the mixture under study has been analyzed, a few general thermodynamic considerations can be helpful. As summarized in Ref. 20, the stability of the thermodynamic-equilibrium states of a system is expressed by the conditions $c_V \geq 0$, $K_T \geq 0$, and $(\partial^2 G / \partial N^2)_{P,T} \geq 0$, where c_V is the heat capacity at constant volume, K_T is the isothermal compressibility, G is the Gibbs free energy, and N is the number of particles. The locus of points where the stability conditions are violated is referred to as the spinodal line, whereas the regions of the state diagram delimited by these lines represent two-phase equilibrium states.

In a binary mixture, the loss of the mechanical stability indicates the onset of an equilibrium between a condensed and an evaporated phase or a condensation/evaporation transition, while the loss of the chemical stability indicates the onset of an equilibrium between two phases with different compositions, or a M/D transition. In the integral equation theory of the phase transitions of binary mixtures, the spinodal lines can be described by finding divergences either in the isothermal compressibility or in the macroscopic composition-composition fluctuations.^{22–24}

TABLE II. Dependence of the Soret coefficient on the temperature at different values of f . Values of the fitting parameter \tilde{T} for the various values of f . The analytic fitting function is $S_T = 1/(T - \tilde{T})$. rms=root-mean-square of the residuals.

f	\tilde{T} (K)	rms
0.2	280.42 ± 1.85	2.3 × 10 ⁻³
0.3	272.31 ± 1.91	1.5 × 10 ⁻³
0.4	245.83 ± 2.45	4.6 × 10 ⁻⁴
0.5	237.51 ± 1.86	5.3 × 10 ⁻⁴
0.6	190.64 ± 0.50	2.7 × 10 ⁻⁴
0.7	144.48 ± 0.11	1.4 × 10 ⁻⁴

In their work, Bhatia and Thornton²⁵ (BT) linked the isothermal compressibility and the density derivative of the Gibbs free energy to the long-wavelength limit of the total number density and composition fluctuations deriving the following relations:

$$S_{NN}(k) = \frac{1}{N} \langle \delta n_k^N \delta n_{-k}^N \rangle \xrightarrow{k=0} n k_B T K_T + \Delta^2 N k_B T / \left(\frac{\partial^2 G}{\partial x_1^2} \right)_{T,P,N}, \quad (10)$$

$$S_{NC}(k) = \frac{1}{N} \langle \delta n_k^N \delta n_{-k}^C \rangle \xrightarrow{k=0} -x_2 x_2 \Delta N k_B T / \left(\frac{\partial^2 G}{\partial x_1^2} \right)_{T,P,N}, \quad (11)$$

$$S_{CC}(k) = \frac{1}{N} \langle \delta n_k^C \delta n_{-k}^C \rangle \xrightarrow{k=0} (x_1 x_2)^{1/2} N k_B T / \left(\frac{\partial^2 G}{\partial x_1^2} \right)_{T,P,N}, \quad (12)$$

where $\delta n_k^{N,C}$ are the Fourier components of the fluctuations and Δ is the dilatation factor defined by $\Delta = n(v_1 - v_2)$, with v_1 and v_2 the partial molar volumes of the two species.

For a binary mixture, these equations, in the form derived from Ornstein–Zernike, can be written as^{20,22}

$$S_{CC}(k) = 1 + n x_1 x_2 [\tilde{h}_{11}(k) + \tilde{h}_{22}(k) - 2\tilde{h}_{12}(k)],$$

$$S_{NN}(k) = 1 + n [x_1^2 \tilde{h}_{11}(k) + x_2^2 \tilde{h}_{22}(k) + 2x_1 x_2 \tilde{h}_{12}(k)],$$

$$S_{NC}(k) = n x_1 x_2 [x_1 \tilde{h}_{11}(k) - x_2 \tilde{h}_{22}(k) + (x_2 - x_1) \tilde{h}_{12}(k)], \quad (13)$$

where n is the total number density, $\tilde{h}_{\alpha\beta}(k)$ is the Fourier transform of the correlation function $h_{\alpha\beta}(r) = g_{\alpha\beta}(r) - 1$, and $g_{\alpha\beta}(r)$ is the radial distribution function.

By knowing that the BT structure factors express the correlations of the total number density and composition fluctuations, as shown in Eqs. (10)–(12), a thermodynamic stability matrix can be constructed, and the precise combination of fluctuations that diverge at $k=0$ can be determined.^{26,27} For all the investigated systems here presented, the incoming divergences in the BT structure factors correspond to a consolute (mixing-demixing) critical transition. This is made evident by the results presented in Figs. 3 and 4. From Fig. 3 it is also observed that by decreasing T , a M/D transition is met for $f=0.7$, while an evaporation/condensation transition is met for $f=0.8$.

It is worth noticing that the strategy here adopted is not well suited for the accurate calculation of phase transitions, which are better described in the grand canonical ensemble. Nevertheless, the aim here is only to have an indication of a possible phase transition with an estimation of the temperature at which it happens and not to precisely compute it.

The values of the inverse of the structure factors, $1/S_{CC}(0)$ versus T , for different values of the parameter f , are shown in Fig. 4, together with the fitting functions $c/(a+T)^b$, which have been used to interpolate the calculated points. The temperatures at which such functions diverge are indicated as the consolute critical temperatures, T_c , and their estimated values are reported in Table III. The difference $|T_c - \tilde{T}|$ is also reported for comparison. The small differences

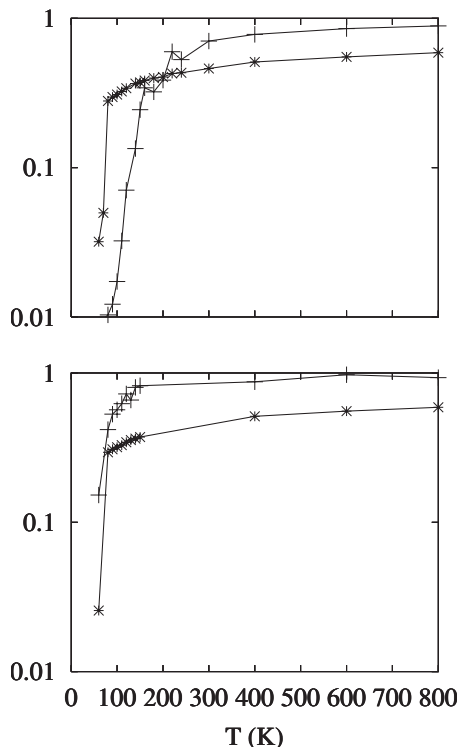


FIG. 3. Comparison of the structure factors S_{NN}^{-1} (“*” symbols) and S_{CC}^{-1} (“+” symbols) vs T for $f=0.7$ (top) and $f=0.8$ (bottom).

between T_c and \tilde{T} clearly show that the temperature dependence of the Soret coefficient for these mixtures can be expressed by the relation

$$S_T(T) = \frac{1}{T - T_c}, \quad (14)$$

where T_c is the consolute (demixing) critical temperature. At very high temperature, where the mixture behaves as a mixture of ideal gas, the $S_T=0$ value is recovered.⁴

This simple dependence of S_T on T is surprising, given that a single property of the mixture, T_c , is involved in this equation. Moreover it is worth paying attention to two aspects of this result. First of all, note that Eq. (14) is not simply a power-law scaling relation, as those discussed in

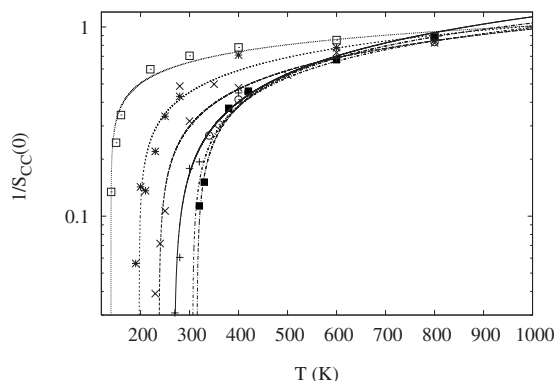


FIG. 4. Inverse of the structure factor, $1/S_{CC}(0)$, vs T for different values of the parameter f . The first line from the right corresponds to $f=0.2$, the other lines to increments 0.1 of f , and the last line (the first from the left) to $f=0.7$.

TABLE III. Consolute critical temperature, T_c , as a function of f computed from EMD simulations and comparison between T_c and \tilde{T} . The temperature difference in kelvin is also reported. rms=root-mean-square of the residuals.

f	T_c (K)	rms	$ T_c - \tilde{T} $ (K)
0.2	314.02 ± 2.253	0.021	34
0.3	291.84 ± 4.605	0.013	19
0.4	269.02 ± 3.037	0.039	23
0.5	244.68 ± 6.973	0.084	7
0.6	197.20 ± 4.578	0.068	7
0.7	139.70 ± 0.556	0.058	5

Sec. I for the cases of mixtures close to the critical temperature^{18,28} and in the classical mean field regime,¹⁹ but a complete equation that allows the calculation of the Soret coefficient once T_c is known. Second, this relation is valid over a broad range of temperatures (of the order of many hundreds of kelvin). This aspect does not hold, for instance, for the scaling rule^{18,28} connecting S_T with the critical temperature, T_c , that is only valid in a close interval around T_c (inside the critical domain).

IV. EQUIMOLAR MIXTURE OF ARGON AND KRYPTON AT $\rho=1.43 \text{ g/cm}^3$

The system described in the previous section has also been considered at a lower density, $\rho=1.43 \text{ g/cm}^3$, for the specific case of $f=0.6$ in order to verify if the simple dependence of the Soret coefficient on the temperature holds also in this case. 750 Argon atoms and 750 Krypton atoms are confined in an orthorhombic periodic cell of size $99 \times 33 \times 33 \text{ \AA}^3$. The time step is again $\Delta t=1 \text{ fs}$, and the chosen cutoff distance, r_c , is 16.5 \AA . The simulations are performed as described in the previous section, and the results are shown in Fig. 5. In particular, S_T diverges at $\tilde{T}=160.99 \text{ K}$ (rms=0.0007), while $\log(S_{CC}(0))$ [interpolated with the function $1/(a+bT)^c$] diverges at $T_c=-a/b=143.75 \text{ K}$ (rms=0.008), with a difference $\tilde{T}-T_c=18 \text{ K}$, which is a satisfactory value. This result confirms that also in this case the Soret coefficient diverges at the demixing temperature of the mixture and that it follows the simple dependence on T found in the previous section.

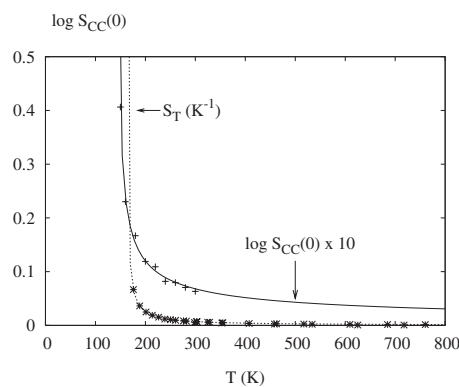


FIG. 5. Logarithm of the structure factor, $\log(S_{CC}(0))$, and Soret coefficient, S_T vs T for a binary equimolar mixture with $f=0.6$ and $\rho=1.43 \text{ g/cm}^3$.

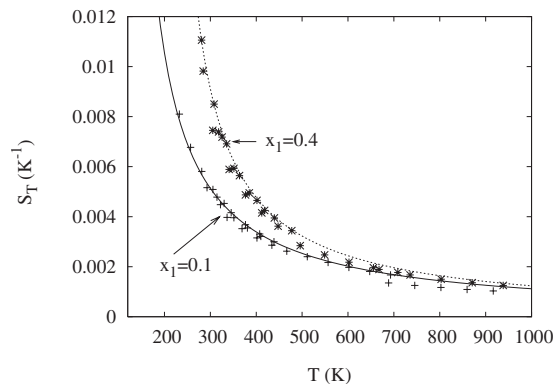


FIG. 6. Dependence of the Soret coefficient on the temperature at $x_1=0.1$ and $x_1=0.4$ with $f=0.6$.

V. DEPENDENCE OF THE SORLET COEFFICIENT FROM THE COMPOSITION OF THE BINARY MIXTURE

In order to further confirm the results obtained in the previous sections for equimolar binary mixtures, different mixtures of Argon- and Krypton-like particles, with the cross term of the LJ interaction potential defined by $\epsilon_{12}=0.6\epsilon_{11}$, have been studied over a wide range of temperatures and compositions. A total number of 1500 particles, with x_1 varying from 0.1 to 0.9, with increments of 0.1 has been considered in an orthorhombic periodic cell of size $89.89 \times 29.96 \times 29.96 \text{ \AA}^3$. For each composition a series of RNEMD simulations at different T_{eq} has been performed as described in Sec. III.

The results of these calculations confirm, at each composition of the mixture, the relation $S_T=1/(T-\tilde{T}(x_1))$, as shown, for example, in Fig. 6 for the cases with $x_1=0.1$ and $x_1=0.4$. The values of \tilde{T} for the different values of x_1 are reported in Table IV.

Also in this case, following the procedure described in Sec. III, the values of \tilde{T} have been compared with the demixing temperatures, T_c , computed from a set of EMD simulations. The values of T_c have been obtained by the interpolation with the functions $c/(a+T)^b$ of the values of $1/S_{CC}(0)$ calculated from EMD simulations at different temperatures. The values of T_c for each composition x_1 are reported in

TABLE IV. Dependence of the Soret coefficient on the temperature at different values of x_1 with $f=0.6$. Values of the fitting parameter \tilde{T} as a function of x_1 . The analytic fitting function is $S_T=1/(T-\tilde{T})$. rms=root-mean-square of the residuals.

x_1	\tilde{T} (K)	rms
0.1	105.2 ± 1.6	0.0002
0.2	144.8 ± 0.8	0.0002
0.3	182.9 ± 0.5	0.0003
0.4	190.1 ± 0.4	0.0004
0.5	190.6 ± 0.5	0.0003
0.6	186.4 ± 0.7	0.0004
0.7	168.4 ± 0.8	0.0003
0.8	143.1 ± 2.4	0.0004
0.9	127.9 ± 1.4	0.0002

TABLE V. Comparison between T_c and \tilde{T} for different values of x_1 , for the mixture with $f=0.6$. The temperature difference in kelvin is also reported. rms=root-mean-square of the residuals.

x_1	T_c (K)	rms	$ T_c-\tilde{T} $ (K)
0.1	120.5 ± 2.94	0.10	15
0.2	150.0 ± 1.62	0.03	4
0.3	168.4 ± 2.77	0.03	14
0.4	197.8 ± 1.55	0.03	8
0.5	197.2 ± 4.58	0.07	7
0.6	179.7 ± 1.27	0.09	7
0.7	158.8 ± 3.40	0.09	9
0.8	148.4 ± 2.37	0.07	10
0.9	120.5 ± 2.94	0.10	7

Table V. The comparison with the values of \tilde{T} further confirms the equivalence, within a reasonable precision, of the two temperatures and therefore the validity of Eq. (14), with, in this case, a composition dependent consolute critical temperature.

An analysis of the dependence of T_c and \tilde{T} on the composition x_1 indicates that the computed values can be well fitted in both cases by a cubic polynomial. This result suggests the possibility of a single bidimensional fitting of all values obtained for S_T , with $f=0.6$ and with different values of T and x_1 , using as fitting function the formula

$$S_T = \frac{1}{[T - \tilde{T}(x_1)]}, \quad (15)$$

with

$$\tilde{T}(x_1) = a + bx_1 + cx_1^2 + dx_1^3. \quad (16)$$

This procedure gives a good fitting of all value, with $a=-40.173$, $b=-760.08$, $c=1128.12$, and $d=-433.87$ for the fitting parameters (rms=0.0004). The fitting function for S_T is depicted in Fig. 7 in a bidimensional plot as a function of both T and x_1 , thus showing that Eq. (15) is able to represent S_T in a wide range of temperatures and compositions. Finally, Fig. 8 shows the values of T_c and \tilde{T} computed at a given composition x_1 (symbols, see Tables IV and V), and the function $\tilde{T}(x_1)$ [full line, Eq. (16)] obtained in the bidimensional fit. One can note a close agreement between the three set of data.

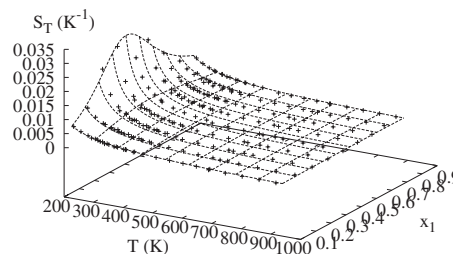


FIG. 7. Dependence of the Soret coefficient on temperature and composition for a binary mixture of Argon- and Krypton-like atoms with $f=0.6$. Fitting function: $\tilde{T}(x_1)=a+bx_1+cx_1^2+dx_1^3$, with $a=-40.173$, $b=-760.08$, $c=1128.12$, and $d=-433.87$ for the fitting parameters and rms=0.0004.

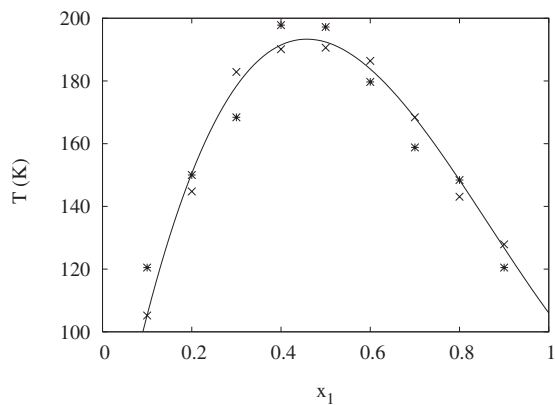


FIG. 8. Consolute critical temperature as a function of the composition for the mixture with $f=0.6$. The points indicated with the * symbol represent the temperatures T_c calculated from the divergence of $S_{cc}(0)$ (see Table V), the points indicated with the “ \times ” symbol represent the temperatures \tilde{T} calculated from the divergence of S_T (see Table IV), and the full line is the function $\tilde{T}(x_1)$ obtained in the bidimensional fitting procedure [Eq. (16)].

The analysis reported in this section further confirms that Eq. (14) well describes the dependence of the Soret coefficient on the temperature even in the case of nonequimolar binary mixtures. In this case the consolute critical temperature is obviously a function of the composition and the dependence of S_T on x_1 is fully included in the dependence of T_c on x_1 .

VI. CONCLUSIONS

The thermodiffusion process in a mixture of Ar- and Kr-like atoms interacting through LJ potentials has been investigated. In a first series of simulations, the Soret coefficient has been computed for an equimolar mixture over a wide range of temperatures (from about 200–1000 K) by changing the cross interaction term, ϵ_{12} . In these simulations, ϵ_{12} has been systematically varied following the relation $\epsilon_{12}=f\epsilon_{11}$, with f assuming values from 0.2 to 0.7 with increments of 0.1. In this way the condition $\epsilon_{12} < \min\{\epsilon_{11}, \epsilon_{22}\}$ is always satisfied; therefore the system presents a M/D phase transition. The values of the Soret coefficient computed from the RNEMD simulations have shown that for each value of the parameter f , a very simple expression relates S_T to the temperature, that is, $S_T=(T-T_c)^{-1}$, where T_c is the demixing critical temperature of the mixture, which increases as f decreases. Lowering the density of the system (by simply increasing the dimensions of the simulation box) does not modify this result and the relation between S_T and T_c still holds.

In a second series of simulations, the dependence of S_T on the mixture composition has been analyzed over a wide range of compositions ($0.1 \leq x_1 \leq 0.9$) and temperature (up to 1000 K) for the specific case with $\epsilon_{12}=0.6\epsilon_{11}$. Also in this

case the simple relation between S_T and T , involving the single parameter T_c , is confirmed. The dependence of S_T on x_1 is included in the dependence of the consolute critical temperature on x_1 . In particular, the computed values of the Soret coefficient have been well fitted with the function $S_T(T, x_1)=[T-(a+bx_1+cx_1^2+dx_1^3)]^{-1}$.

Work is in progress in our laboratories in order to verify if this simple relation is valid also for other mixtures showing consolute critical phenomena. Moreover, further work is planned to exploit the behavior of $S_T(T, x_1)$ in the phase diagram region characterized by values of $f > 0.7$ for which condensation–evaporation transitions occur. Finally, it is also planned the extension of the presented method to interaction potentials able to describe the structure of colloidal suspensions, for which experimental data on the behavior of S_T as a function of the molar composition have been produced.^{29,30}

ACKNOWLEDGMENTS

This work has been carried out with the financial support of the “Regione Autonoma della Sardegna” and of the University of Ferrara.

- ¹C. Ludwig, *Sitzungsber. Akad. Wiss. Wien, Math.-Naturwiss. Kl.* **20**, 539 (1856).
- ²C. Soret, *Arch. Sci. Phys. Nat.* **3**, 48 (1879).
- ³S. Chapman and T. G. Cowling, *The Mathematical Theory of Non-Uniform Gases* (Cambridge University Press, Cambridge, 1970).
- ⁴K. I. Morozov, *Phys. Rev. E* **79**, 031204 (2009).
- ⁵K. Harstad, *Ind. Eng. Chem. Res.* **48**, 6907 (2009).
- ⁶E. Leonardi, B. D’Aguanno, and C. Angeli, *J. Chem. Phys.* **128**, 054507 (2008).
- ⁷L. Kincaid and B. Hafskold, *Mol. Phys.* **82**, 1099 (1994).
- ⁸J. M. Kincaid, M. Lopez de Haro, and E. G. D. Cohen, *J. Chem. Phys.* **79**, 4509 (1983).
- ⁹S. N. Rasuli and R. Golestanian, *Phys. Rev. Lett.* **101**, 108301 (2008).
- ¹⁰R. Piazza, *Soft Matter* **4**, 1740 (2008).
- ¹¹D. Reith and F. Müller-Plathe, *J. Chem. Phys.* **112**, 2436 (2000).
- ¹²J. Luettmer-Strathmann, *Lect. Notes Phys.* **584**, 24 (2002).
- ¹³M. A. Anisimov, E. E. Gorodetskii, V. D. Kulikov, and J. V. Sengers, *Pis'ma Zh. Eksp. Teor. Fiz.* **60**, 522 (1994); *JETP Lett.* **60**, 535 (1994).
- ¹⁴F. Müller-Plathe, *J. Chem. Phys.* **106**, 6082 (1997).
- ¹⁵A. P. Lyubartsev and A. Laaksonen, *Comput. Phys. Commun.* **128**, 565 (2000).
- ¹⁶P. Bordat, D. Reith, and F. Müller-Plathe, *J. Chem. Phys.* **115**, 8978 (2001).
- ¹⁷A. Voit, A. Krekhov, and W. Köhler, *Phys. Rev. E* **76**, 011808 (2007).
- ¹⁸M. Giglio and A. Vendramini, *Phys. Rev. Lett.* **34**, 561 (1975).
- ¹⁹W. Enge and W. Köhler, *Phys. Chem. Chem. Phys.* **6**, 2373 (2004).
- ²⁰B. D’Aguanno and C. Nardone, *Il Nuovo Cimento D* **16**, 1205 (1994).
- ²¹A. Kamimura and N. Ito, *J. Phys. Soc. Jpn.* **77**, 125001 (2008).
- ²²G. Malescio, *Phys. Rev. A* **42**, 2211 (1990).
- ²³G. Malescio, *Phys. Rev. A* **42**, 6241 (1990).
- ²⁴M. C. Abramo and C. Caccamo, *Phys. Lett. A* **166**, 70 (1992).
- ²⁵A. B. Bhatia and D. E. Thornton, *Phys. Rev. B* **2**, 3004 (1970).
- ²⁶X. S. Chen and F. Forstmann, *J. Chem. Phys.* **97**, 3696 (1992).
- ²⁷L. Strigari, M. Rovere, and B. D’Aguanno, *J. Chem. Phys.* **105**, 2020 (1996).
- ²⁸L. Mistura, *Il Nuovo Cimento B* **12**, 35 (1972).
- ²⁹R. Piazza and A. Parola, *J. Phys.: Condens. Matter* **20**, 153102 (2008).
- ³⁰H. Ning, J. K. G. Dhont, and S. Wiegand, *Langmuir* **24**, 2426 (2008).